

# Magnetic and Junction Properties of Half-Metallic Double-Perovskite Thin Films

H. Asano, N. Koduka, K. Imaeda, M. Sugiyama, and M. Matsui

Department of Crystalline Materials Science, Nagoya University, Furo-cho, Chikusa-ku, Nagoya 464-8603, Japan

**This paper reports the magnetic, electrical, and microstructural properties of epitaxial thin films with an ordered double-perovskite structure.  $\text{Sr}_2\text{FeMoO}_6$  (SFMO) and  $\text{Sr}_2\text{CrReO}_6$  (SCRO) films have been grown by sputtering onto the lattice-matched substrates of  $\text{Ba}_{0.4}\text{Sr}_{0.6}\text{TiO}_3$ -buffered and bare  $\text{SrTiO}_3$ , respectively. These films exhibit high saturation magnetization  $M_s$  values ( $3.8 \mu_B/\text{f.u.}$  for SFMO and  $0.9 \mu_B/\text{f.u.}$  for SCRO), which are close to the expected values for their half-metallicity, and high Curie temperature  $T_c$  values (385 K for SFMO and 620 K for SCRO). Surface analyzes by AFM and XPS indicate that these films have atomically flat and well-defined surfaces, which are free from any surface precipitates. This enables us to employ a standard photolithographic process for fabricating magnetic tunnel junctions based on these films. SFMO junctions with a native barrier formed by surface oxidation of a SFMO base-electrode and a Co counterelectrode have shown a tunnel magnetoresistance ratio of 10% at 4.2 K.**

*Index Terms*—Double perovskite, epitaxial film, half-metallic ferromagnet, magnetic tunnel junction.

## I. INTRODUCTION

**O**RDERED double-perovskites  $\text{Sr}_2\text{FeMoO}_6$  (SFMO),  $\text{Sr}_2\text{CrReO}_6$  (SCRO), and related materials, having a half-metallic nature and a high Curie temperature  $T_c$  (420 K for SFMO and 635 K for SCRO [1], [2]), have attracted much attention both due to their rich physics and their potential spintronic applications. For polycrystalline samples of these materials, large room-temperature magnetoresistance has been observed, which arises from spin-polarized tunneling through the insulating grain boundary [1], [2]. In a simple picture, the local moments of SFMO are carried by the localized majority-spin electrons on  $\text{Fe}^{3+}$  ( $3d^5$ ,  $S = 5/2$ ) ions, while the conduction band is occupied by the minority-spin electrons on  $\text{Mo}^{5+}$  ( $4d^1$ ,  $S = 1/2$ ) ions [1]. The  $\text{Fe}^{3+}$  ( $S = 5/2$ ) and  $\text{Mo}^{5+}$  ( $S = 1/2$ ) ions order on alternately on the perovskite B-sites and the respective spins couple antiferromagnetically. Similar picture is expected for SCRO with  $\text{Cr}^{3+}$  ( $3d^3$ ,  $S = 3/2$ ) and  $\text{Re}^{5+}$  ( $5d^2$ ,  $S = 1$ ) ions. In a perfectly ordered structure, theoretical spin-only saturation magnetic moments of  $4 \mu_B/\text{f.u.}$  and  $1 \mu_B/\text{f.u.}$  are expected for SFMO and SCRO, respectively. It has been shown that the magnetization and  $T_c$  depend strongly on the degree of the B-site ordering in these materials [3]. Since the most applications require thin film multilayer structures, high-quality epitaxial films with highly-ordered structures and well-defined surfaces are essentially important.

It has been shown from previous studies that one often finds difficulties in preparing epitaxial thin films of these double-perovskite materials. These difficulties are possibly related to the coexistence of the multivalent transition metal species, which results in a narrow window of film growth in these materials. In fact, it has been reported that the undesirable features of SFMO films including reduced  $M_s$  and  $T_c$  values, outgrowths, and surface precipitates [4]–[8], which prevent the fabrication of magnetic tunnel junctions with the use of a conventional photolithographic technique.

In this paper, we will report on the magnetic and electrical characterization as well as the surface analysis of sputtered SFMO and SCRO films. In addition, fabrication and properties of magnetic tunnel junctions (MTJ) with a SFMO base-electrode will also be presented.

## II. EXPERIMENTAL PROCEDURE

All thin films were deposited using a magnetron sputtering technique. Details of our film growth have been reported previously [9], [10]. The substrate used was polished (001) and (111) surfaces of  $\text{SrTiO}_3$ , which has a lattice mismatch of  $-1.0$  and  $0.1\%$  to SFMO and SCRO, respectively. As a buffer layer for SFMO,  $\text{Ba}_{0.4}\text{Sr}_{0.6}\text{TiO}_3$  (BSTO) films of 50 nm in thickness were grown on STO at a temperature of  $700^\circ\text{C}$ . After annealing in air at  $900$ – $1150^\circ\text{C}$  for 1 h in order to relieve epitaxial strain induced by STO substrates, we obtained BSTO layers with the lattice constants of  $0.3943$ – $0.3948$  nm, of which lattice mismatch to SFMO is as low as  $-0.1\%$ . SFMO films were grown at temperatures of  $800^\circ\text{C}$  in a 76 mTorr Ar+5% $\text{H}_2$  sputtering gas. SCRO films were grown at a temperature of  $700^\circ\text{C}$  in a 76 mTorr Ar+0.5% $\text{H}_2$  sputtering gas. Typical thickness of SFMO and SCRO films in this study was 100 nm.

The orientation, phase purity, in-plane and out-of plane lattice spacing and ordering of the perovskite B-site for the films were examined by two circle and four circle X-ray diffraction (XRD) with  $\text{CuK}\alpha$  radiation. Here, to describe the B-site ordering of the double-perovskite structure, we used the long-range order parameter  $S$ , which was calculated from the relative intensity of the (111) superlattice peak to that of the (222) fundamental peak for (111) epitaxial films. In this notation,  $S = 1$  and  $0$  corresponds to the perfectly-ordered and random cases, respectively.

## III. RESULTS AND DISCUSSION

In order to optimize magnetic properties in epitaxial double-perovskite films, we have systematically investigated the effect of the B-site ordering in (111) epitaxial films. The dependences of long-range order parameter  $S$  on substrate temperature  $T_s$

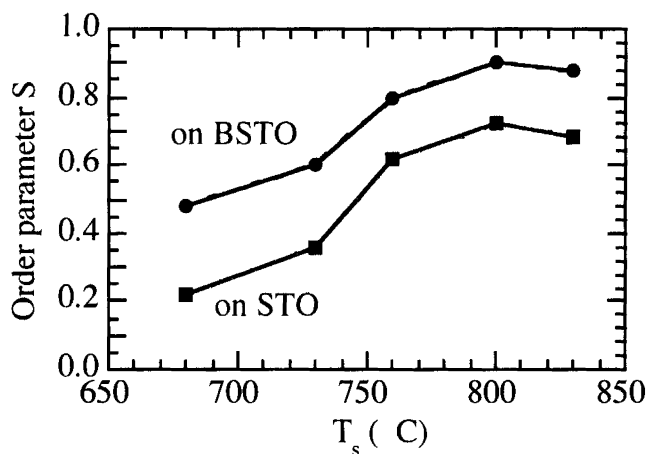


Fig. 1. Order parameter  $S$  as a function of substrate temperatures for SFMO films on BSTO-buffered (111) STO and on bare (111) STO substrates.

for SFMO (111) films are shown in Fig. 1. Here, the results are presented for films grown on BSTO-buffered (111) STO, as well as films on bare (111) STO. It is found that at the same  $T_s$  SFMO films on BSTO always exhibit larger  $S$  values than SFMO films on STO. Although the reason why the  $S$  values are improved by the introduction of BSTO buffer layer is not clear, the growth mode of SFMO films on the lattice-matched layer may play an important role. Regarding  $T_s$  dependence for each type of SFMO films, the maximum  $S$  values were obtained at  $T_s = 800^\circ\text{C}$ , and with lower  $T_s$  the  $S$  values decrease. The maximum  $S$  value of 0.9 was obtained for SFMO films on BSTO at  $T_s = 800^\circ\text{C}$ . Considering that the  $S$  value has relation to occupancy  $g$  of the Fe atoms on one sublattice of the perovskite B-site with  $S = 2g - 1$ ,  $S = 0.90$  is equivalent to  $g = 0.95$ , that is, the antisite defect of 0.05. Similar investigations on SCRO films have been conducted, and  $S$  values larger than 0.9 were obtained for SCRO films on STO at  $T_s = 700^\circ\text{C}$ .

It was found that both (001) and (111) films simultaneously grown in the same run showed very similar magnetic properties. For the remainder of this paper, therefore, we will concentrate on the results for (001) SFMO and SCRO films grown under the optimal conditions. XRD analyzes indicated that these films were of high phase purity of a double-perovskite structure without any detectable second phases. The out-of plane lattice constants for SFMO films on BSTO, which were calculated from the XRD data, were 0.7888–0.7891 nm, which is in good agreement to the bulk c-axis lattice constant of 0.7888 nm [1]. The out-of plane lattice constant for SCRO film on STO was 0.7834–0.7842 nm, which is comparable to or slightly (0.2%–0.3%) larger than the bulk c-axis lattice constant of 0.7820 nm [2].

Fig. 2 shows temperature dependences of saturation magnetization  $M_s$  measured at  $H = 10\text{ kOe}$  for SFMO and SCRO films. The saturation magnetization  $M_s$  value at 77 K is  $3.8\ \mu_B/\text{f.u.}$  and  $0.9\ \mu_B/\text{f.u.}$  for SFMO and SCRO films, respectively. These values are close to the respective half-metallic values of  $4\ \mu_B/\text{f.u.}$  and  $1\ \mu_B/\text{f.u.}$ . The ferromagnetic Curie temperature  $T_c$  for the SCRO films is around 620 K, which is much higher than that (385 K) for the SFMO films. These  $T_c$  values are slightly lower than the respective values of the bulk materials.

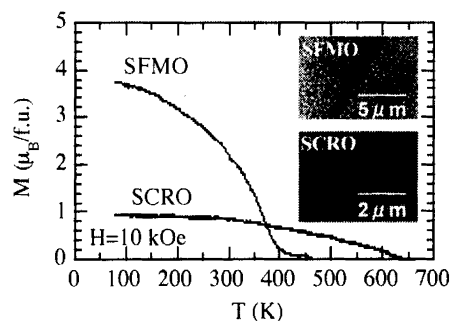


Fig. 2. Magnetization versus temperature curves for SFMO and SCRO films. The inset shows AFM images for SFMO and SCRO films.

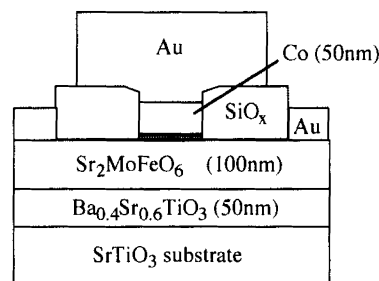


Fig. 3. Schematic drawing of a MTJ device in a cross-sectional view. The junction area is  $30 \times 30\ \mu\text{m}^2$ .

Since the surface properties of films are essentially important for application to multi-layer tunneling devices, ex-situ surface characterization on these films has been performed by means of AFM and XPS. AFM images for SFMO and SCRO films are shown in the inset in Fig. 2. The surface roughness (root-mean-square, Rms) over these areas is as small as 1.1 and 0.4 nm for SFMO and SCRO films, respectively. The average grain (or domain) size is about 500 and 50 nm for SFMO and SCRO films, respectively. It should be noted that AFM scans over a wide area ( $15 \times 15\ \mu\text{m}^2$ ) of the samples can never detect the out-growth structures and/or  $\text{FeO}_x$  particles, which have been often observed for SFMO films grown by pulsed laser deposition [8], [9]. For our SFMO films the absence of the magnetic  $\text{FeO}_x$  particles, of which  $T_c$ s are much higher than that of SFMO, was also confirmed by the results of the temperature-dependent magnetization as shown in Fig. 2.

Finally, we will present the results of MTJ with SFMO films. Fig. 3 shows a schematic diagram of the fabricated MTJ devices. Tunneling multilayers with a 100-nm-thick double-perovskite base-electrode, a native barrier, which was formed by air oxidation for 1 month of a base-electrode film, and a 50-nm-thick Co were deposited on BSTO-buffered STO substrates. Junction delineation has been done by means of standard UV lithography and ion milling. Fig. 4 shows the magnetic field dependence of the resistance for a Co/I/SFMO junction with a junction area of  $30 \times 30\ \mu\text{m}^2$ , measured at 4.2 K. A definite tunnel magnetoresistance effect is observed, and the measured MR ratio is 10%. To our knowledge, this is the first observation of TMR effect in micron-sized SFMO junctions defined by standard photolithography. This result indicates the existence of an insulating native barrier on the air-exposed SFMO surface. The possible origin of the insulating native barrier is due either to trapping of the

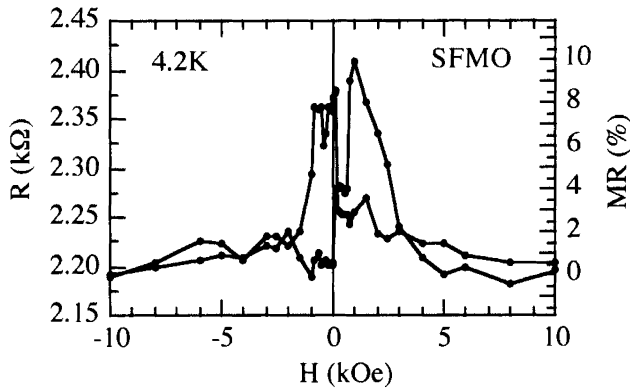


Fig. 4. Magnetic field dependence of the resistance for a Co/I/SFMO junction at 4.2 K.

itinerant  $4d$ -carriers in the  $\text{Sr}_2\text{FeMoO}_{6+\delta}$  surface with excess oxygen  $\delta$  [11] or to formation of a  $\text{SrMoO}_4$  (insulating) phase [12]. In order to obtain information of the surface chemistry of the SFMO film surface, *ex-situ* XPS analysis were conducted on several film samples stored in air for different periods after film deposition. However, at present, the possible origin of the insulating native barrier could not be identified from the XPS data. Moreover, the low TMR ratio may be related to the quality of the native barrier or to the chemistry of the interface between the base-electrode and the native barrier. Further study is necessary to understand the detailed nature of the surface of double-perovskite materials and improve their tunneling properties.

#### IV. CONCLUSION

We have succeeded in sputter-deposition of SFMO and SCRO epitaxial films with superior magnetic properties as well as atomically flat and well-defined surfaces. Using standard

photolithography, magnetic tunnel junctions with a SFMO base electrode, a native barrier, which is formed by surface oxidation of a base electrode, and a Co counterelectrode are fabricated, showing 10% MR ratio at 4.2 K. The present results, although preliminary, suggest that sputtered double-perovskite films with excellent magnetic and microstructural properties are useful for constructing MTJ with all double-perovskite electrodes.

#### REFERENCES

- [1] K. I. Kobayashi, T. Kimura, H. Sawada, K. Terakura, and Y. Tokura, *Nature*, vol. 395, pp. 677–679, 1998.
- [2] H. Kato, T. Okuda, Y. Okimoto, Y. Tomioka, Y. Takenoya, A. Ohkubo, M. Kawasaki, and Y. Tokura, *Appl. Phys. Lett.*, vol. 81, pp. 328–330, 2002.
- [3] Li. Balcels, J. Navarro, M. Bibes, A. Roig, B. Martinez, and J. Fontcuberta, *Appl. Phys. Lett.*, vol. 78, pp. 781–783, 2001.
- [4] T. Manako, M. Izumi, Y. Konishi, K.-I. Kobayashi, M. Kawasaki, and Y. Tokura, *Appl. Phys. Lett.*, vol. 74, pp. 2115–2217, 1999.
- [5] H. Asano, S. B. Ogale, J. Garrison, A. Orozco, Y. H. Li, E. Li, V. Smolyaninova, C. Galley, M. Downes, M. Rajeswari, R. Ramesh, and T. Venkatesan, *Appl. Phys. Lett.*, vol. 74, pp. 3696–3698, 1999.
- [6] H. Q. Yin, Z. S. Zou, J. P. Zhou, R. I. Dass, and J. B. Goodenough, *Appl. Phys. Lett.*, vol. 75, pp. 2812–2814, 1999.
- [7] M. Besse, F. Pailloux, A. Barthelemy, K. Bouzehouane, A. Fert, J. Olivier, O. Durand, F. Wyezisk, R. Bisaro, and J.-P. Contour, *J. Cryst. Growth*, vol. 241, pp. 448–451, 2002.
- [8] M. Bibes, K. Bouzehouane, A. Barthelemy, M. Besse, S. Fusil, M. Bowen, P. Seneor, J. Carrey, V. Cros, A. Vaures, J.-P. Contour, and A. Fert, *Appl. Phys. Lett.*, vol. 83, pp. 2629–2631, 2003.
- [9] H. Asano, M. Kohara, and M. Matsui, *Jpn. J. Appl. Phys.*, vol. 41, pp. L1081–L1083, 2002.
- [10] H. Asano, H. Koduka, A. Tsuzuki, and M. Matsui, *Appl. Phys. Lett.*, vol. 85, pp. 263–265, 2004.
- [11] S. Agata, Y. Moritomo, A. Machida, K. Katoh, and A. Nakamura, *Jpn. J. Appl. Phys.*, vol. 41, pp. L688–0, 2002.
- [12] D. Niebieskikwiat, A. Caneiro, R. D. Sanchez, and J. Fontcuberta, *Phys. Rev. B*, vol. 64, pp. 180 406-1–180 406-4, 2001.

Manuscript received February 6, 2005.